

Clickable Degradable Aliphatic Polyesters via Copolymerization with Alkyne Epoxy Esters: Synthesis and Postfunctionalization with Organic Dyes

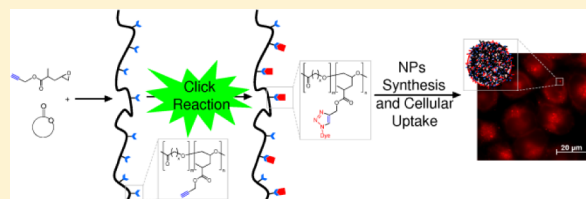
Nele S. Teske,[†] Julia Voigt,[†] and V. Prasad Shastri^{*,†,‡}

[†]Institute for Macromolecular Chemistry, Hermann Staudinger Haus, University of Freiburg, Stefan-Meier Str. 31, 79104 Freiburg, Germany

[‡]BIOSS Centre for Biological Signalling Studies, University of Freiburg, Schänzlestr. 18, 79104 Freiburg, Germany

S Supporting Information

ABSTRACT: Degradable aliphatic polyesters are the cornerstones of nanoparticle (NP)-based therapeutics. In this paradigm, covalent modification of the NP with cell-targeting motifs and dyes can aid in guiding the NP to its destination and gaining visual confirmation. Therefore, strategies to impart chemistries along the polymer backbone that are amenable to easy modification, such as 1,3-dipolar cycloaddition of an azide to an alkyne (the “click reaction”), could be significant. Here we present a simple and efficient way to introduce alkyne groups at high density in aliphatic polyesters without compromising their crystallinity via the copolymerization of cyclic lactones with propargyl 3-methylpentenoate oxide (PMPO). Copolymers of lactic acid and ϵ -caprolactone with PMPO were synthesized with up to 9 mol % alkyne content, and accessibility of the alkyne groups to the click reaction was demonstrated using several dyes commonly employed in fluorescence microscopy and imaging (Cy3, ATTO-740, and coumarin 343). In order to establish the suitability of these copolymers as nanocarriers, copolymers were formulated into NPs, and cytocompatibility, cellular uptake, and visualization studies undertaken in HeLa cells. Dye-modified NPs exhibited no quenching, remained stable in solution for at least 10 days, showed no cytotoxicity, and were readily taken up by HeLa cells. Furthermore, in addition to enabling the incorporation of multiple fluorophores within the same NP through blending of individual dye-modified copolymers, dye-modified polyesters offer advantages over physical entrapment of dye, including improved signal to noise ratio and localization of the fluorescence signal within cells, and possess the necessary prerequisites for drug delivery and imaging.



INTRODUCTION

Aliphatic polyesters derived from cyclic lactones [ϵ -caprolactone (ϵ CL), lactide and glycolide] represent the major family of polymers currently used in medical applications. These applications range from implantable and injectable drug delivery systems^{1–4} to support structures (porous scaffolds) for cell seeding and cultivation to coatings for medical devices.^{5–10} In recent years, copolymers of lactide and glycolide have seen extensive use in the development of injectable nanoparticles (NPs) for targeted therapy and imaging.^{11,12} To increase the utility of degradable polyesters for targeted therapeutics, much effort has focused on developing monomers bearing chemistries suitable for functionalization with homing peptides, antibodies, and/or imaging agents. Two approaches have been explored to date: (1) synthesis of lactone derivatives possessing functional groups that are amenable to postfunctionalization^{13–15} and (2) direct functionalization of the nanoparticle, device, or scaffold surface by combining for example controlled hydrolysis of the surface with carbodiimide coupling of the desired chemical entity.¹⁶ Although the latter approach ensures that the desired information is indeed on the surface of the nanoparticle, this methodology for modification may be incompatible with the application or chemistry of the polymer,

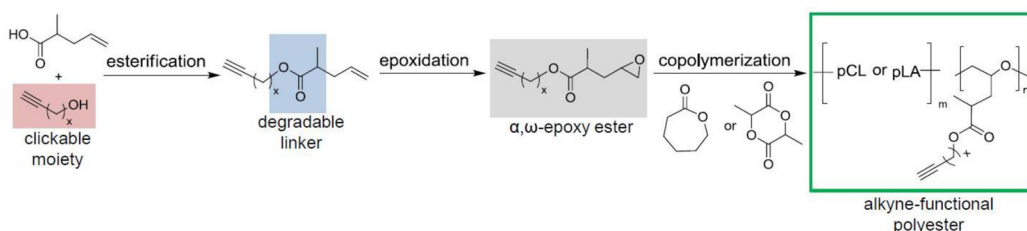
as solvents can swell the polymer matrix or destabilize the nanoparticle suspension and compromise end use. While the synthesis of functionalized lactones is time-consuming and often plagued with low yields, methods that are much easier to implement have been reported, including the chain-end modification route¹⁴ and direct functionalization of the polymer backbone.^{17–19} Nevertheless, systems that combine ease of synthesis with simple predictable coupling chemistries can enhance the application space of these polyesters.

With regard to functional groups that might be considered for further biofunctionalization, the “click reaction” involving 1,3-dipolar cycloaddition of azides with alkyne groups features prominently,²⁰ as it is an atom-economical synthetic route that can be quantitative under the right conditions. Bertozzi and co-workers demonstrated that with strained cyclooctynes, 1,3-dipolar cycloaddition in almost quantitative yields without the need for copper(II) catalysts can be achieved.²¹ There are several reports in the literature on the synthesis of aliphatic polyesters bearing azide or alkyne groups via copolymerization of derivatized lactones.^{22–27} Alkyne groups provide unique

Received: June 12, 2014

Published: June 27, 2014

Scheme 1. General Scheme for the Synthesis of Alkyne Epoxy Esters and Alkyne-Functionalized Aliphatic Polyesters



access to simple chemistry to introduce dyes and contrast agents for imaging applications. However, in order to benefit from the simplicity of click chemistry, systems that can be easily realized is the key. While most lactone synthesis involves complex synthetic methodology,²² the work by Emrick and co-workers^{26,27} stands out as it employs the copolymerization of α -propargyl- δ -valerolactone, which is easily accessible, to synthesize alkyne-modified poly(ϵ -caprolactone) (pCL). However, the synthesis of other alkyne-bearing variants of valerolactone, such as those possessing degradable linkers, is not trivial. In a recent publication, we reported the functionalization of polyesters using α,ω -epoxy esters.^{28,29}

This approach offers two advantages over other published methods: (1) since epoxides can undergo ring-opening polymerization (ROP), the use of α,ω -epoxy esters allows the introduction of a variety of groups through simple dicarboxylic diimide coupling that are now linked to the parent polymer backbone via degradable ester linkages; (2) ring opening of the epoxide results in a substituted poly(ethylene glycol) (PEG)-like backbone that can be deemed biocompatible.³⁰ In this study, the introduction of alkyne ester groups along the pCL and poly(*dl*-lactide) (pLA) backbone using the alkyne epoxy ester propargyl 3-methylpentenoate oxide (PMPO) is presented (Scheme 1), and the postfunctionalization of these polymers with a variety of organic dyes that have utility in functional imaging is demonstrated. As a step toward their application in targeted therapeutics, the polymers were formulated into nanoparticles, and their cellular compatibility was evaluated.

RESULTS AND DISCUSSION

Synthesis of α,ω -Epoxy Ester Monomer. The premonomer propargyl 3-methylpentenoate (PMP) was synthesized in quantitative yield by esterification of propargyl alcohol (PA) with 2-methyl-4-pentenoic acid using *N,N'*-dicyclohexylcarbodiimide and 4-(dimethylamino)pyridine. Trace amounts of dicyclohexylurea were removed during the final workup using flash chromatography. The purity of the premonomer was confirmed by ¹H NMR analysis (Figure 1A, spectrum 3) and elemental analysis. The epoxidation was carried out using a molar excess of Oxone under buffered conditions at near-neutral pH to preserve the ester bond in PMP. The overall conversion efficiency was around 62%. However, recovery of the unreacted PMP educt during purification and further epoxidation resulted in quantitative conversion. ¹H NMR analysis (Figure 1A, spectrum 4) revealed that the alkyne group remained unreacted, indicating selective epoxidation of the terminal vinyl group. This was further verified by IR analysis (Figure 1B), where a clear signal at 3300 cm⁻¹ for the alkyne C–H vibration of PMPO is observed, which proves the presence of an alkyne functional group in the epoxide.

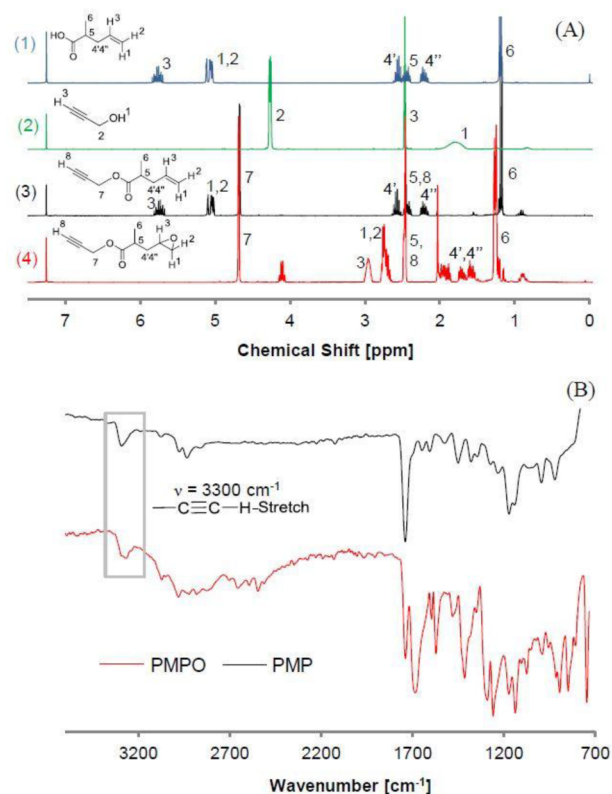


Figure 1. Comparisons of (A) ¹H NMR and (B) IR spectra of the vinyl premonomer (black) and the functionalized epoxide (red).

Copolymerization of PMPO with ϵ CL and LA. To establish the generality of alkyne epoxy esters for modification of the aliphatic polyester backbone, copolymerization of PMPO with ϵ CL and 3,6-dimethyl-1,4-dioxane-2,5-dione (LA) was investigated. The chemical structures of the expected copolymers are shown in Scheme 1. The polymerization conditions were chosen to yield polymers with number-average molecular weights (M_n) in the range of 8000 to 10 000 g/mol. This molecular weight range was chosen because it is suitable for the production of nanoparticles via the nanoprecipitation method^{31,32} for targeted therapeutics and imaging. Typical ¹H NMR spectra of the copolymers of PMPO with ϵ CL and LA are shown in Figure 2. NMR analysis showed the presence of intact alkyne protons in both copolymers (Figure 2, peak assignment g, δ = 5.2 and 5.4 ppm, respectively).

Optimization of the Copolymerization Conditions. Typical copolymerizations of the α,ω -epoxy esters with cyclic lactones have been carried out at 130 °C using Sn(Oct)₂ and benzyl alcohol (BnOH) as the initiator system.²⁹ However, the presence of the alkyne bond in the comonomer warranted a study to establish the most optimal temperature for the

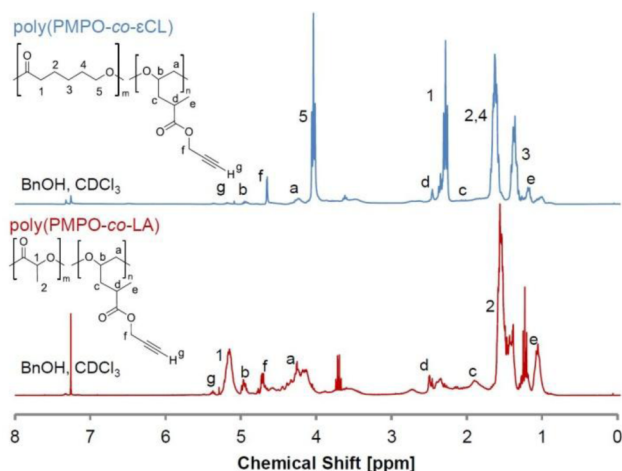


Figure 2. ^1H NMR spectra of copolymers of PMPO with ϵCL (blue) and LA (red). The PMPO content in the copolymers was 8%.

copolymerization. The findings of this study are summarized in Table 1. It is clear that a lower polymerization temperature of

Table 1. Optimization of the Copolymerization Conditions^a

copolymer	T [$^{\circ}\text{C}$]	M_n (SEC) [10^3 g/mol]	PDI	M_n^b [10^3 g/mol]
poly(PMPO-co-LA)	90	5.1	1.6	8.2
	130	3.3	1.7	8.2
poly(PMPO-co- ϵCL)	90	7.8	1.4	12.0
	130	5.2	1.6	12.0

^aThe $\epsilon\text{CL}/\text{PMPO}$ or LA/PMPO ratio was set to a theoretical value of 90:10, and the polymerization was carried out for 24 h. ^bTheoretical molecular weight calculated on the basis of an initiator/monomer ratio of 1/100.

90 $^{\circ}\text{C}$ was still capable of affording polymers with the desired molecular weight without an appreciable increase in the polydispersity index (PDI). The PDI values of 1.4–1.7 were in the range of what is expected from ROP and are indicative of a relatively narrow molecular weight distribution.³³ Interestingly, the copolymers with ϵCL had higher M_n than the copolymers with LA. This may be attributed to a difference in kinetics due to the higher ring strain in the ϵCL monomer.³⁴

PMPO Incorporation Efficiency and Its Effect on Copolymer Molecular Weight. The linear density of biologically relevant information is important for many applications such as cellular targeting and imaging, as this affects the efficiency with which a system can interrogate a cell in the former case and the signal-to-noise ratio in the latter. Although Emrick and co-workers^{26,27} reported greater than 25 mol % incorporation of α -propargyl- δ -valerolactone into a pCL backbone, in general one limiting factor in the modification of aliphatic polyester backbones through copolymerization with derivatized lactones such as depsipeptides has been the poor incorporation³⁵ of the functional monomer. Therefore, a study to understand the incorporation of PMPO in both ϵCL and LA copolymers was undertaken using feed ratios between 5 and 30 mol %. Furthermore, these feed ratios were chosen because past studies have shown that beyond 30 mol % the polymer molecular weights are severely diminished. The results for the incorporation of PMPO into the polymer backbone are shown in Figure 3.

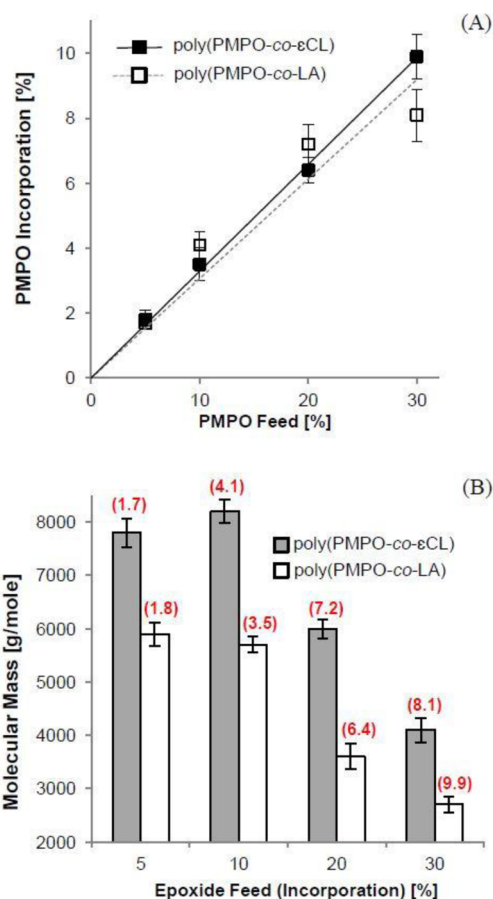


Figure 3. (A) PMPO incorporation efficiency and (B) dependence of the copolymer mass on PMPO for two different copolymers. In (B), the numbers in parentheses are the mol % incorporation of the epoxide in the copolymer.

The PMPO incorporation was estimated using the ^1H NMR integration by comparing the integrals of the alkyne protons with those of methylene protons from the ϵCL backbone (Figure 2 top, peak assignment 5, $\delta = 4.04$ ppm) or the methine protons of the LA unit (Figure 2 bottom, peak assignment 1, $\delta = 5.17$ ppm). As expected, increasing the epoxide monomer in the feed leads to increased incorporation, with a maximum incorporation of around 10%. The lack of a one-to-one correlation between the feed ratio and the composition in the copolymer can be attributed to the poor self-reactivity of the α,ω -epoxy ester monomer as reported earlier.²⁹ However, with higher incorporation, a decrease in molecular weight and yield is observed, and this is consistent with past reports²⁹ (Table S1 in the Supporting Information).

The incorporation in the α,ω -epoxy ester system is less than what was reported by Emrick and co-workers, where the similarity in cyclic ring structure between ϵCL and valerolactone may have favored cross-reactivity between the monomers, which is necessary for high incorporation. However, in the system reported by Emrick, high incorporation comes at the expense of crystallinity, as these copolymers are viscous solids at room temperature. In contrast while α,ω -epoxy esters have poor self-reactivity, they have good cross-reactivity with cyclic lactones and result in copolymers with a well-defined statistical distribution of epoxy ester units;²⁹ more importantly, they retain the thermal characteristics of the pCL or pLA backbone, as discussed later. Thus, this system nevertheless

yields copolymers of degradable aliphatic polyesters with a high incorporation of clickable acetylene groups with narrow PDI and acceptable molecular weights that are in the range suitable for nanoparticle synthesis.³²

Thermal Characteristics of Copolymers. Since the intended application of these polymers is in injectable nanoparticle systems, stability of the polymers both during storage and use is a prerequisite. Therefore, the thermal behavior of the copolymers was investigated to gain insights into the changes in physical properties in comparison with pure polyester. The decomposition temperatures (T_d) of the copolymers were in the ranges of 333–360 °C for poly(PMPO-*co*- ϵ CL) and 238–251 °C for poly(PMPO-*co*-LA), which are comparable to the T_d values of the homopolymers (pCL, 346 °C; pLA, 252 °C), suggesting that the copolymers do not have any deficit in thermal stability in comparison with the homopolymers. Differential scanning calorimetry analysis revealed a decrease in the glass transition temperature (T_g) for the copolymers in comparison with the homopolymers (Table 2). The homopolymers of ϵ CL and LA synthesized under the

Table 2. Thermal Properties of Alkyne-Functionalized Copolymers

copolymer	PMPO in copolymer [mol %]	T_g [°C]	T_m [°C]	T_d [°C]
poly(PMPO- <i>co</i> - ϵ CL)	0	-61	59	346
	2	-59	50	359
	4	-57	50	360
	8	-51	40	333
	10	-28	138	238
poly(PMPO- <i>co</i> -LA)	0	42	147	252
	2	41	143	251
	4	39	142	248
	10	28	138	238

polymerization conditions possessed T_g values of -58 and 42 °C, respectively, which are consistent with literature reports.^{36,37} However, in the copolymers with greater than 8% incorporation of PMPO, a significant shift in T_g to lower values [-67 and 28 °C for poly(PMPO-*co*- ϵ CL) and poly(PMPO-*co*-LA), respectively] was observed. This is an expected outcome, as both backbone substitution and lower molecular weight would promote polymer chain flexibility and backbone rotation, both of which contribute to lowering of T_g .³⁸ However, at 10 mol % incorporation in the pLA system, the T_g is significantly below physiological temperature. This may prove valuable because functional polymers that undergo softening when introduced into a physiological environment could be used to leverage NP shape in delivery into cells.³⁹

Modification of Copolymers by Click Reaction: Proof-of-Principle Study Using Organic Dyes. Having demonstrated that clickable groups can be incorporated into the polymer backbone, it is important that these groups are accessible for derivatization. Toward this objective, a study was undertaken to investigate the click reactions between poly(PMPO-*co*-LA) and several organic dyes (Figure 4A).

As a first example, the reaction of the copolymer (3.8 mol % alkyne groups) with 3-azido-7-hydroxycoumarin (7-HC), a dye that becomes fluorescent upon conversion to the triazole derivative, was investigated. In this system, the appearance of fluorescence provides direct confirmation of the formation of the 1,3 bipolar adduct and hence quantification of the click reaction. The ¹H NMR spectrum of the clicked 7-HC

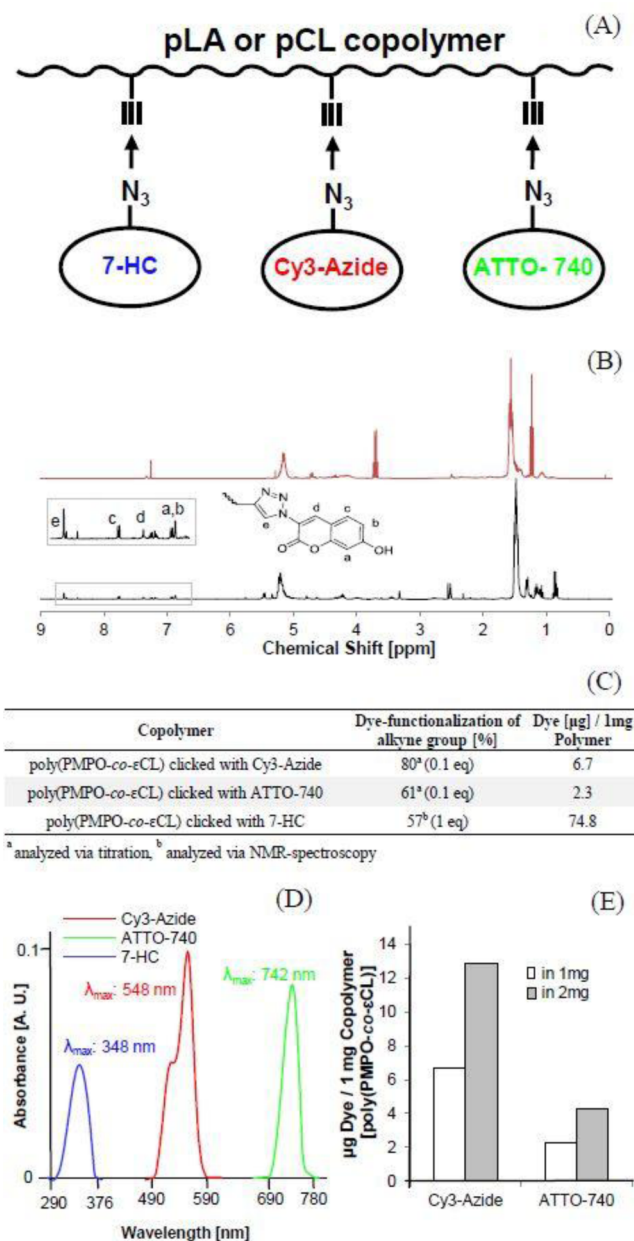


Figure 4. (A) Schematic of copolymers clicked with different organic dyes. (B) Comparison of the ¹H NMR spectra of poly(PMPO-*co*-LA) before (red) and after (black) the click reaction with 7-HC (conversion ~57%). (C) Summary of the conversion efficiencies of the click reactions with various dyes. The concentrations of the dyes along the polymer backbone were determined from calibration curves over a concentration range of 2–50 μ g (Figure S4 in the Supporting Information). (D) Example UV-vis spectra of dye-modified copolymer systems. Values shown next to the peaks are λ_{max} values for the dyes clicked to the copolymer; the λ_{max} values for the free dyes are 552 nm for Cy3-Azide and 740 nm for Atto740. (E) Plot showing linear scaling of the fluorescence intensity of the dye-modified copolymers.

copolymer conjugate (Figure 4B) clearly showed signals corresponding to the newly formed 1,2,3-triazole ring (peak assignments a–e), and additionally, this click modification showed >50% efficiency (i.e., conversion of the alkyne groups), indicating good accessibility of the alkyne moieties to chemical modification in solution.

To elaborate this to other organic dyes that have utility in cell and functional imaging, click reactions of poly(PMPO-*co*- ϵ CL) (2 mol % alkyne groups) with azide-functionalized cyanine 3 (Cy3) and ATTO-740 were studied. These dyes were chosen because they have different adsorption ($\lambda_{\text{abs}}^{\text{Cy3}} = 552 \text{ nm}$, $\lambda_{\text{abs}}^{\text{ATTO-740}} = 740 \text{ nm}$) and emission ($\lambda_{\text{em}}^{\text{Cy3}} = 570 \text{ nm}$, $\lambda_{\text{em}}^{\text{ATTO-740}} = 764 \text{ nm}$) wavelengths. Furthermore, while Cy3 is widely used in cell imaging, ATTO-740 is a near-infrared dye that is suitable for functional fluorescence imaging. The conversion efficiency (i.e., the ratio of the molar equivalents of dye on the polymer backbone to the initial dye concentration) is summarized in Figure 4C. Conversions as high as 80% could be achieved with the Cy3-Azide system. The ability to accomplish derivatization of the copolymer backbone with a variety of organic dyes was verified by UV-vis spectroscopy (Figure 4D). The excellent correspondence between the absorption maxima of the Cy3- and ATTO-740-conjugated polymers and those of the free dyes suggests the absence of any dye quenching upon covalent immobilization, which was also confirmed by the linear scaling of the adsorption as a function of polymer concentration (Figure 4E). The absence of any drastic change in molecular weight or an increase in PDI upon copolymer functionalization (Table S2 in the Supporting Information) is suggestive of minimal degradation during modification.

Cytocompatibility of Dye-Functionalized Nanoparticles. In order to ascertain the suitability of these novel dye-functionalized copolymers for injectable and imaging applications, dye-functionalized pCL copolymers were formulated into NPs using the single-step nanoprecipitation method.³² Independent of the dye modification, all three copolymers yielded stable NPs that exhibited size distributions that are acceptable for injectable applications⁴⁰ and comparable zeta potentials (Table 3) and showed good stability even after 10

Table 3. Overview of Synthesized Nanoparticles^a

copolymer	size [nm] (<i>n</i> = 3)	zeta potential [mV]
poly(PMPO- <i>co</i> - ϵ CL)	140 ± 2	-27 ± 3
poly(PMPO- <i>co</i> - ϵ CL) clicked with Cy3-Azide	138 ± 10	-7 ± 1
poly(PMPO- <i>co</i> - ϵ CL) clicked with ATTO-740	150 ± 22	-24 ± 7
poly(PMPO- <i>co</i> - ϵ CL) clicked with 7-HC	130 ± 10	-11 ± 3
poly(PMPO- <i>co</i> - ϵ CL) with all three dyes blended	160 ± 15	-28 ± 5

^aConcentration of polymer 0.5% (w/v) (5 ng/mL).

days, with a maximum size change of 10% (Table S3 in the Supporting Information). Furthermore, blending of the single-dye-functionalized copolymers (Figure 5A) afforded NPs possessing multiple chromophores without compromising the size and surface charge characteristics. NPs bearing multiple distinct spectral signatures can be useful in optically coded systems for diagnostics or imaging based on optical multiplexing.

Utility of Dye-Functionalized NPs for Imaging in Vivo.

Toward the application of these copolymers in targetable therapeutics and imaging, the cytotoxicity of the NPs in HeLa cells was studied. The viabilities of HeLa cells incubated with 7-HC-, Cy3-Azide-, and ATTO-740-modified NPs at different concentrations of 0.025, 0.125, and 0.5 mg/mL after 24 h of incubation are shown in Figure 5B. Even at the highest NP

concentration of 0.5 mg/mL, a high cell viability of 80% was observed, suggesting that the dye-modified copolymers have good cytocompatibility.

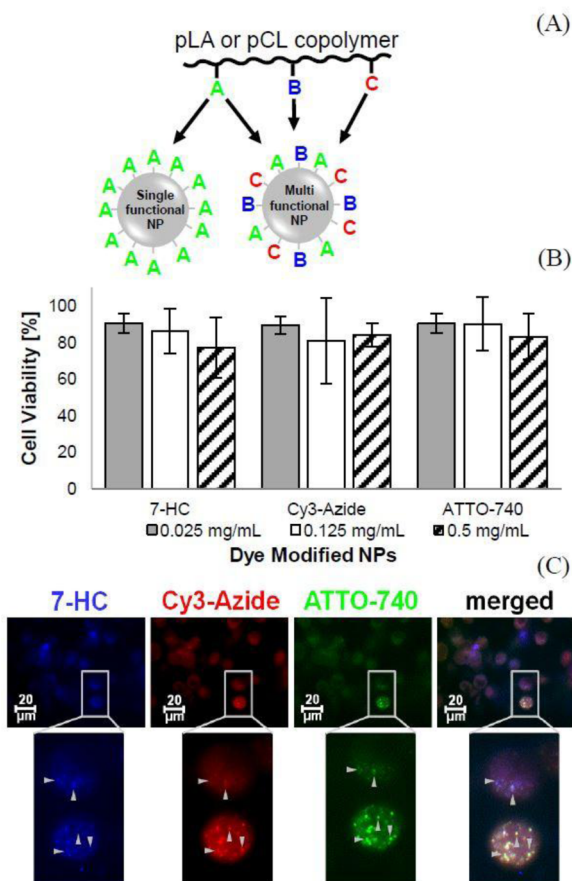


Figure 5. Cytocompatibility of dye-labeled NPs: (A) Schematic showing NPs synthesized from single-dye-labeled copolymers and a blend of three individually labeled copolymers. (B) Viability of HeLa cells in the presence of dye-labeled NPs as determined using MTT assay after 24 h of incubation. The results are reported as values normalized to cell viability on tissue-culture plastic. (C) Fluorescence microscopy images of HeLa cells incubated with NPs produced by blending of three copolymers individually labeled with 7-HC, Cy3-Azide, and ATTO-740. For comparison, images of HeLa cells incubated with single-dye (Cy3 or 7-HC)-functionalized NPs are shown in Figure S5 in the Supporting Information.

The visualization of fluorescent signals emanating from all three dyes in a single NP system was explored by incubating HeLa cells with NPs prepared from a blend of three single-dye-functionalized copolymers: 7-HC, Cy3-Azide and ATTO-740 (Figure 5C). It is evident that the NPs can be clearly visualized within the cells in all three respective fluorescence channels, indicating that the excitation and emission are not impacted by the presence of multiple fluorophores with the NPs. This bodes well for the exploration of these polymers for the development of imaging and diagnostic probes.

In cellular and tissue imaging, the ability to accurately superimpose the information from various modalities can provide exceptional functional information.⁴¹ This is achieved using nanoprobe information that can be interrogated by multiple modalities such as magnetic resonance imaging, X-ray computer tomography, and fluorescence imaging.⁴² Polymers are particularly well suited for fashioning such

nanoprobes as they can be tailored to carry a plurality of agents. In the conventional approach, the fluorescent molecules are encapsulated in a nanocarrier along with other agents. In this scenario, leakage of the fluorescent molecule beyond the confines of the nanocarrier can confound the acquisition and assignment of information. In this context, advantages that covalent immobilization of the dye can confer over the conventional approach of encapsulation are higher signal-to-noise ratio and improved localization of the fluorescence. To explore this premise, coumarin 343 (C-343), a dye with very high affinity for cell lipids, was incorporated into NPs through encapsulation and click-chemistry modification, and the distributions of fluorescence in HeLa cells were examined after 2 h. First, we observed that in comparison with NPs prepared from polymers with covalently immobilized C-343, encapsulation of C-343 resulted in a 60% increase in NP size (Figure 6A), which is not desirable because size can profoundly

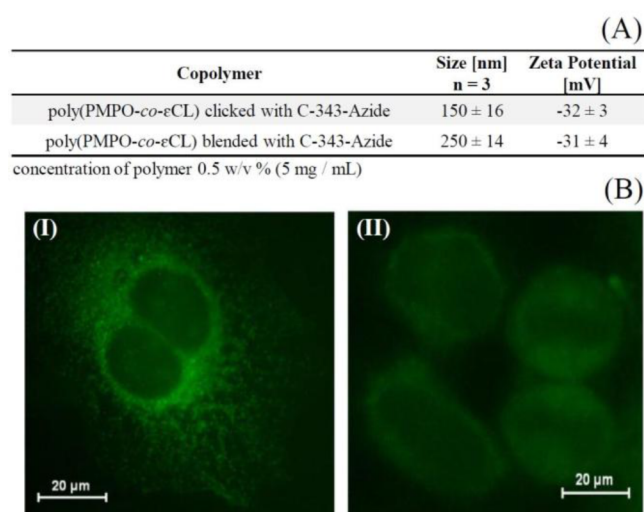


Figure 6. C-343-dye-functionalized NPs: (A) Size and zeta potential of clicked and blended C-343-functionalized NPs. (B) Fluorescence microscopy images of HeLa cells coincubated with C-343-dye-functionalized NPs: (I) dye covalently bonded; (II) dye blended into the copolymer.

impact biodistribution.⁴³ However, more significantly, fluorescence microscopy revealed that while the fluorescence in cells incubated with NPs with encapsulated dye was feeble and dispersed throughout the cell, in contrast the fluorescence in cells treated with NPs with covalently immobilized dye showed highly punctate, intense fluorescence that was remarkably confined to the cytosol, with very negligible staining of the cell-membrane lipids (Figure 6B).

SUMMARY

A new approach for the synthesis of aliphatic degradable polyesters with a high density of alkyne functionality has been presented. The accessibility of the pendant alkyne functional groups to solution-phase click chemistry has been demonstrated using various fluorescent organic dyes that have broad utility in cell and tissue imaging. This class of dye-functionalized polyesters possesses good cytocompatibility and offers potential advantages over conventional systems for the development of nanoprobes for cellular and tissue imaging.

ASSOCIATED CONTENT

Supporting Information

Experimental methods and characterization, synthetic details for preparation of 7-HC, overview of alkyne-functionalized copolymers, calibration curves for Cy3-Azide and ATTO-740 to calibrate the concentrations of the dyes along the polymer backbone, molecular weights and PDI values for unmodified and dye-functionalized copolymers, stability studies of NPs sizes (comparison of day 1 to day 10), and fluorescence microscopy images of HeLa cells coincubated with single-dye-functionalized NPs. This material is available free of charge via the Internet at <http://pubs.acs.org>.

AUTHOR INFORMATION

Corresponding Author

prasad.shastri@gmail.com

Notes

The authors declare no competing financial interest.

ACKNOWLEDGMENTS

The authors thank Carina Knittel and Esther Kohler for assistance and Dr. Ulrike Shastri for careful reading of the manuscript. This work was funded by the Fifth INTERREG Upper Rhine Program (Project A21: NANO@MATRIX), the Excellence Initiative of the German Federal and State Governments (Grant EXC 294, Centre for Biological Signalling Studies), and the University of Freiburg.

REFERENCES

- Shoichet, M. S. *Macromolecules* **2010**, *43*, 581–591.
- Kroeze, R. J.; Helder, M. N.; Govaert, L. E.; Smit, T. H. *Materials (Basel)* **2009**, *2*, 833–856.
- Shin, H.; Jo, S.; Mikos, A. G. *Biomaterials* **2003**, *24*, 4353–4364.
- Sinha, V. R.; Bansal, K.; Kaushik, R.; Kumria, R.; Trehan, A. *Int. J. Pharm.* **2004**, *278*, 1–23.
- Duncan, R. *Nat. Rev. Drug Discovery* **2003**, *2*, 347–360.
- Freed, L. E.; Vunjak-Novakovic, G.; Biron, R. J.; Eagles, D. B.; Lesnoy, D. C.; Barlow, S. K.; Langer, R. *Nat. Biotechnol.* **1994**, *12*, 689–693.
- Nair, L. S.; Laurencin, C. T. *Prog. Polym. Sci.* **2007**, *32*, 762–798.
- Langer, R. *Acc. Chem. Res.* **2000**, *33*, 94–101.
- Uhrich, K. E.; Cannizzaro, S. M.; Langer, R. S.; Shakesheff, K. M. *Chem. Rev.* **1999**, *99*, 3181–3198.
- Meng, F.; Zhong, Z.; Feijen, J. *Biomacromolecules* **2009**, *10*, 197–209.
- Mundargi, R. C.; Babu, V. R.; Rangaswamy, V.; Patel, P.; Aminabhavi, T. M. *J. Controlled Release* **2008**, *125*, 193–209.
- Lee, S.; Jeong, J.; Shin, S.; Kim, J.; Chang, Y.; Kim, J. *J. Magn. Magn. Mater.* **2004**, *276*, 2432–2433.
- Albertsson, A.-C.; Varma, I. K. *Biomacromolecules* **2003**, *4*, 1466–1486.
- Xu, L.; Zhang, Z.; Wang, F.; Xie, D.; Yang, S.; Wang, T.; Feng, L.; Chu, C. J. *Colloid Interface Sci.* **2013**, *393*, 174–181.
- Cheng, Y.; Hao, J.; Lee, L. A.; Biewer, M. C.; Wang, Q.; Stefan, M. C. *Synthesis* **2012**, *44*, 2163–2173.
- Guo, J.; Gao, X.; Su, L.; Xia, H.; Gu, G.; Pang, Z.; Jiang, X.; Yao, L.; Chen, J.; Chen, H. *Biomaterials* **2011**, *32*, 8010–8020.
- El Habnoui, S.; Darcos, V.; Coudane, J. *Macromol. Rapid Commun.* **2009**, *30*, 165–169.
- Nottelet, B.; El Ghzaoui, A.; Coudane, J.; Vert, M. *Biomacromolecules* **2007**, *8*, 2594–2601.
- Ponsart, S.; Coudane, J.; Vert, M. *Biomacromolecules* **2000**, *1*, 275–281.
- Kolb, H. C.; Finn, M. G.; Sharpless, K. B. *Angew. Chem., Int. Ed.* **2001**, *40*, 2004–2021.

- (21) Baskin, J. M.; Prescher, J. A.; Laughlin, S. T.; Agard, N. J.; Chang, P. V.; Miller, I. A.; Lo, A.; Codelli, J. A.; Bertozzi, C. R. *Proc. Natl. Acad. Sci. U.S.A.* **2007**, *104*, 16793–16797.
- (22) Lu, C.; Shi, Q.; Chen, X.; Lu, T. *J. Polym. Sci., Part A: Polym. Chem.* **2007**, *45*, 3204–3217.
- (23) Riva, R.; Schmeits, S.; Stoffelbach, F.; Jérôme, C.; Jérôme, R.; Lecomte, P. *Chem. Commun.* **2005**, 5334–5336.
- (24) Silvers, A. L.; Chang, C.-C.; Emrick, T. *J. Polym. Sci., Part A: Polym. Chem.* **2012**, *50*, 3517–3529.
- (25) Maji, S.; Zheng, M.; Agarwal, S. *Macromol. Chem. Phys.* **2011**, *212*, 2573–2582.
- (26) Parrish, B.; Breitenkamp, R. B.; Emrick, T. *J. Am. Chem. Soc.* **2005**, *127*, 7404–7410.
- (27) Cooper, B. M.; Emrick, T. *J. Polym. Sci., Part A: Polym. Chem.* **2009**, *47*, 7054–7065.
- (28) Shastri, V. P. U.S. Patent 6,730,722 B2, 2004.
- (29) Wurth, J. J.; Shastri, V. P. *J. Polym. Sci., Part A: Polym. Chem.* **2013**, *51*, 3375–3382.
- (30) Knop, K.; Hoogenboom, R.; Fischer, D.; Schubert, U. S. *Angew. Chem., Int. Ed.* **2010**, *49*, 6288–6308.
- (31) Schneider, J.; Jallouk, A. P.; Vasquez, D.; Thomann, R.; Forget, A.; Pino, C. J.; Shastri, V. P. *Langmuir* **2013**, *29*, 4092–4095.
- (32) Sussman, E. M.; Clarke, M. B.; Shastri, V. P. *Langmuir* **2007**, *23*, 12275–12279.
- (33) Dechy-Cabaret, O.; Martin-Vaca, B.; Bourissou, D. *Chem. Rev.* **2004**, *104*, 6147–6176.
- (34) Saiyasombat, W.; Molloy, R.; Nicholson, T. M.; Johnson, A. F.; Ward, I. M.; Poshyachinda, S. *Polymer* **1998**, *39*, 5581–5585.
- (35) Barrera, D. A.; Zylstra, E.; Lansbury, P. T.; Langer, R. *J. Am. Chem. Soc.* **1993**, *115*, 11010–11011.
- (36) Labet, M.; Thielemans, W. *Chem. Soc. Rev.* **2009**, *38*, 3484–3504.
- (37) Garlotta, D. *J. Polym. Environ.* **2002**, *9*, 63–84.
- (38) Tieke, B. *Makromolekulare Chemie*; Wiley-VCH: Weinheim, Germany, 2005.
- (39) Yoo, J.; Mitragotri, S. *Proc. Natl. Acad. Sci. U.S.A.* **2010**, *107*, 11205–11210.
- (40) Voigt, J.; Christensen, J.; Shastri, V. P. *Proc. Natl. Acad. Sci. U.S.A.* **2014**, *111*, 2942–2947.
- (41) Vonwil, D.; Christensen, J.; Fischer, S.; Ronneberger, O.; Shastri, V. P. *Mol. Imaging Biol.* **2013**, *16*, 350–361.
- (42) Baker, M. *Nature* **2010**, *463*, 977–980.
- (43) Gaumet, M.; Vargas, A.; Gurny, R.; Delie, F. *Eur. J. Pharm. Biopharm.* **2008**, *69*, 1–9.